

## Critical Froude number for transition from a steady to an unsteady plane fountain injected into a homogeneous fluid

N. Srinarayana<sup>1</sup>, S. W. Armfield<sup>1</sup>, M. Behnia<sup>1</sup> and Wenxian Lin<sup>2</sup>

<sup>1</sup>School of Aerospace, Mechanical and Mechatronic Engineering,  
The University of Sydney, NSW 2006, Australia

<sup>2</sup>School of Engineering and Physical Sciences,  
James Cook University, Townsville, QLD 4811, Australia

### Abstract

In this paper, we present the critical Froude number for unsteadiness at full development of plane fountains with parabolic velocity inlet profile. Numerical investigations are conducted over the range of Reynolds number,  $6 \leq Re \leq 120$ . The critical Froude number for transition from a steady to unsteady flow varies with the Reynolds number. For  $Re \gtrsim 60$ , the transition is independent of  $Re$  and is nearly constant at a Froude number of  $Fr \sim 1.0$ . Over the range  $6 < Re \lesssim 50$ , there is a significant increase in the transition Froude number.

### Introduction

A fountain, also known as a negatively buoyant jet, is formed whenever a fluid is injected upwards into a lighter fluid, or downward into a denser fluid. In both cases, buoyancy opposes the momentum of the ejected flow until the jet penetrates a finite distance and falls back towards the source.

The behavior of plane fountains is governed by the Reynolds, Froude, and Prandtl numbers, defined as,

$$\begin{aligned} Re &\equiv \frac{V_{in} X_{in}}{\nu}, \\ Fr &\equiv \frac{V_{in}}{\sqrt{g(\rho_{in} - \rho_{\infty})/\rho_{\infty} X_{in}}} \\ &\equiv \frac{V_{in}}{\sqrt{g\beta(T_{\infty} - T_{in}) X_{in}}}, \\ Pr &\equiv \frac{\nu}{\kappa}, \end{aligned} \quad (1)$$

where  $X_{in}$  and  $V_{in}$  are the half-width and average velocity at the fountain source respectively,  $\nu$  is the kinematic viscosity of the fountain fluid,  $g$  is the acceleration due to gravity,  $\rho_{in}$  and  $T_{in}$  are the density and temperature of the fountain fluid at the source,  $\rho_{\infty}$  and  $T_{\infty}$  are the density and temperature of the ambient fluid,  $\kappa$  is the thermal diffusivity, and  $\beta$  is the coefficient of volumetric expansion, respectively. The second expression of the Froude number in equation (1) applies when the density difference is due to the difference in temperature of the fountain and ambient fluid using the Oberbeck–Boussinesq approximation. A schematic of a typical fountain is shown in figure 1, where a lighter fluid is injected upwards into denser fluid. The fountain, after attaining a maximum height, flows downward and outward along the floor and settles at a lesser penetration height of  $Z_m$ .

The early work on fountains began with Morton [1] who obtained an analytical solution for the fountain penetration height. This work was later extended by Campbell and Turner [2] and Baines *et al.* [3], who conducted experiments on both round and planar turbulent fountains. Recently, Williamson *et al.* [4] conducted extensive experimental studies on low-Reynolds number round fountain behaviors and

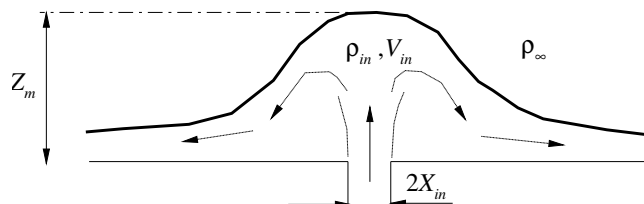


Figure 1: Schematic of a fountain.

classified fountain flows in various regimes. Lin and Armfield [5, 6] numerically investigated the effect of the Reynolds number on the height of planar fountains over the  $0.2 \leq Fr \leq 1.0$  and  $Re \leq 200$ .

Srinarayana *et al.* [7] experimentally studied different flow regimes and instability modes for low  $Re$  plane fountains. There is, however, very little information on critical Froude number for unsteadiness of planar fountains. The current work is a direct extension of Srinarayana *et al.* [8], who obtained numerically the critical Froude number for unsteadiness in the fountain flow with a uniform velocity profile at the inlet as  $Fr = 2.25$  at the single Reynolds number  $Re = 100$ . In this paper, we present the transition Froude number of planar fountains with parabolic velocity profile at the inlet for Reynolds numbers in the range  $6 \leq Re \leq 120$ .

### Numerical model

The physical system considered here is a rectangular box filled with a fluid between the insulated top (ceiling) and bottom (floor) solid walls which are distance  $H$  apart. The fluid is initially still and isothermal at a temperature  $T_{\infty}$ . The fountain source is a slot of width  $2X_{in}$  in the center of the floor. For  $t > 0$  the fluid issues from the slot with a temperature  $T_{in} < T_{\infty}$  and a parabolic velocity profile

$$V = V_m \left[ 1 - \left( \frac{X}{X_{in}} \right)^2 \right], \quad (2)$$

where  $V_m$  is the maximum velocity of the parabolic profile, equal to  $1.5V_{in}$  for a fully developed laminar flow. The discharge conditions are maintained thereafter. The flow is assumed to remain two-dimensional. The computational domain is sketched in figure 2. The temperature difference between the source and ambient fluids results in the required buoyancy. The governing equations are the incompressible Navier–Stokes and energy equations with the Oberbeck–Boussinesq approximation for buoyancy. The following equations are written in conservative, non-dimensional form in Cartesian co-

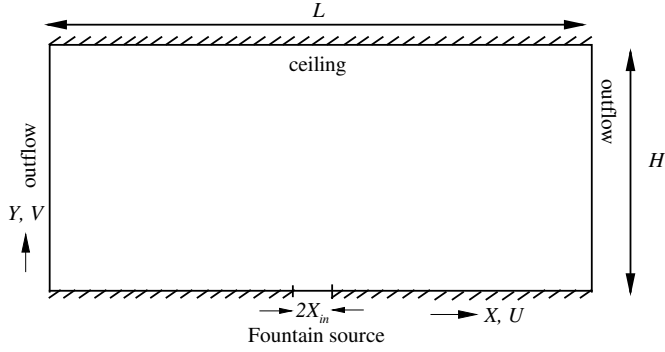


Figure 2: Computational domain.

ordinates,

$$\frac{\partial u}{\partial x} + \frac{\partial v}{\partial y} = 0, \quad (3)$$

$$\frac{\partial u}{\partial \tau} + \frac{\partial(uu)}{\partial x} + \frac{\partial(vu)}{\partial y} = -\frac{\partial p}{\partial x} + \frac{1}{Re} \left( \frac{\partial^2 u}{\partial x^2} + \frac{\partial^2 u}{\partial y^2} \right), \quad (4)$$

$$\frac{\partial v}{\partial \tau} + \frac{\partial(uv)}{\partial x} + \frac{\partial(vv)}{\partial y} = -\frac{\partial p}{\partial y} + \frac{1}{Re} \left( \frac{\partial^2 v}{\partial x^2} + \frac{\partial^2 v}{\partial y^2} \right) + \frac{1}{Fr^2} \theta, \quad (5)$$

$$\frac{\partial \theta}{\partial \tau} + \frac{\partial(u\theta)}{\partial x} + \frac{\partial(v\theta)}{\partial y} = \frac{1}{RePr} \left( \frac{\partial^2 \theta}{\partial x^2} + \frac{\partial^2 \theta}{\partial y^2} \right). \quad (6)$$

The following non-dimensionalisation is used:

$$\begin{aligned} x &= \frac{X}{X_{in}}, y = \frac{Y}{X_{in}}, u = \frac{U}{V_{in}}, v = \frac{V}{V_{in}}, \\ \tau &= \frac{t}{(X_{in}/V_{in})}, p = \frac{P}{\rho V_{in}^2}, \theta = \frac{T - T_{\infty}}{T_{in} - T_{\infty}}, \end{aligned} \quad (7)$$

with  $x, y = 0$  at the fountain source centre.

The initial and boundary conditions are,

$$u = v = \theta = 0 \text{ when } \tau < 0, \quad (8)$$

and when  $\tau \geq 0$ ,

$$\frac{\partial u}{\partial x} = 0, \frac{\partial v}{\partial x} = 0, \frac{\partial \theta}{\partial x} = 0 \text{ on } x = \pm L/(2X_{in}), \quad (9)$$

$$u = 0, v = 1.5(1 - x^2), \theta = -1 \text{ on } |x| \leq 1, y = 0, \quad (10)$$

$$u = v = 0, \frac{\partial \theta}{\partial y} = 0 \text{ on } |x| > 1, y = 0, \quad (11)$$

$$u = v = 0, \frac{\partial \theta}{\partial y} = 0 \text{ on } |x| \leq L/(2X_{in}), y = H/X_{in}, \quad (12)$$

respectively. The results are obtained using the open source code Gerris [9]. The computational domain is  $-100 \leq x \leq +100$  and  $0 \leq y \leq 100$ . The minimum grid spacing is  $4.88 \times 10^{-4}$  in each direction. The mesh is dynamically adapted based on the vorticity and the temperature. The adaptive refinement is performed at the fractional time-step. The number of cells also varies with  $Fr$  due to the adaptive nature of the algorithm. As an example, the mesh size for  $Fr = 2.0$  at  $Re = 100$  is 114750 cells.

## Results

The results have been obtained for Reynolds numbers ranging from  $6 \leq Re \leq 120$  and at a fixed Prandtl number of  $Pr = 7$ .

The difference between a steady and unsteady fountain at full development is demonstrated with time-evolution of fountains for  $Fr = 1.17$  and  $Fr = 1.2$  at  $Re = 60$  and  $Pr = 7$ , shown in figure 3. After the fountain is initiated, it travels upwards until momentum balances buoyancy, when it comes to rest. The rising fluid spreads due to its reduced velocity and interaction with the ambient fluid. The descending fluid then interacts with the environment and with the upflow, restricting the rise of further fluid. The descending fluid, heavier than the ambient, moves along the floor as a gravity current. The fountain is symmetric and steady for  $Fr = 1.17$  at full development whereas the fountain starts symmetrically for  $Fr = 1.2$ , but eventually becomes unsteady and asymmetric. An interesting feature is the flapping, i.e. lateral oscillation, that can be observed for  $Fr = 1.2$  in figure 3. The flapping phenomenon can be thought of as a lateral movement of the fountain fluid on either side of the fountain source. At the extreme of each oscillation the top of the fountain is shed laterally exposing the core of the fountain. The fountain then increases in height and the process is again repeated on the other side.

The time series of non-dimensional penetration heights for the Froude numbers  $Fr = 1.17$  and  $Fr = 1.2$  at  $Re = 60$  and  $Pr = 7$  are shown in figure 4. The fountain height in the current work is defined as the vertical distance from floor along the centre line to the location where the local temperature excess  $(T - T_{\infty})$  drops to 10% of the inlet excess  $(T_{in} - T_{\infty})$ . This definition is similar to that used by Goldman and Jaluria [10] in their experiments on free-fountains. The fountain height is non-dimensionalised by the half-width of the inlet manifold  $X_{in}$ . The fountain height at full development in figure 4 does not vary with time for the Froude number  $Fr = 1.17$ . The unsteady and periodic nature of the side to side oscillations of the flow in the flapping fountain is clearly seen in the periodic structure of the corresponding fountain height at  $Fr = 1.2$ , observed in figure 4.

## Discussion

The critical Froude numbers for transition at full development for  $6 \leq Re \leq 120$  are mapped onto a  $Re - Fr$  plot, shown in figure 5, along with the previous experimental observations of Srinarayana *et al.* [7].

The transition Froude number at any Reynolds number was obtained by testing for different Froude number and is the lowest Froude number at which the fountain flaps about the fountain source. The critical Froude numbers are well approximated with,

$$Fr \sim 0.95 + 490 Re^{-2} \quad (13)$$

The critical  $Fr$  line obtained here agrees well with the experimental results [7]. As seen the critical Froude number for unsteadiness at full development varies with the Reynolds number. For  $Re \gtrsim 60$ , the transition Froude number is nearly constant at  $Fr \sim 1.0$ ; for  $10 < Re \lesssim 50$ , there is a steady increase in the transition Froude number; and for  $Re \lesssim 10$ , there is a very sharp increase in the transition Froude

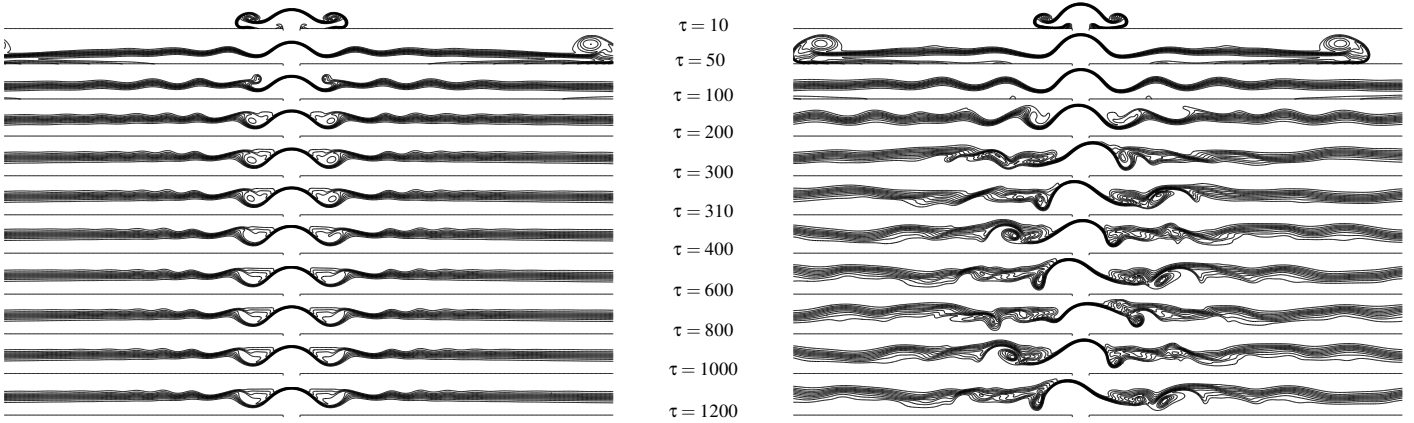


Figure 3: Evolution of temperature fields for  $Fr = 1.17$  (left column) and  $Fr = 1.2$  (right column) at  $Re = 60$  and  $Pr = 7$ .

number. It is noted that Srinarayana *et al.* [7] used three different fits to describe the critical Froude number line, that is, for  $Re \gtrsim 60$  they used  $Fr \sim 1.0$ , for  $10 < Re \lesssim 50$  they used  $FrRe^{2/3} = 13$ , and for  $Re \lesssim 10$  they used  $Fr \sim Re^{-n}$ , where  $n \approx 2$  to 4. In the current paper, it is shown that the critical  $Fr$  line is well approximated with a single curve.

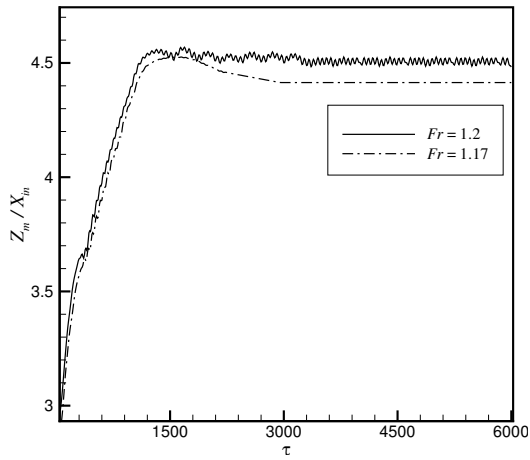


Figure 4: Time-series of non-dimensional fountain height for  $Fr = 1.17$  and  $Fr = 1.2$  at  $Re = 60$  and  $Pr = 7$ .

It is also noted that the critical Froude number for transition to unsteady flow obtained here for  $Re \gtrsim 60$  matches well with the experimental results of Friedman *et al.* [11] for  $Re \gtrsim 55$ . For non-circular fountain source, their  $Fr$  was based on the inlet hydraulic diameter,  $D_H = 4A_c/P_m$ , where  $A_c$  is the cross-sectional area and  $P_m$  is the perimeter. For an inlet with a long span compared to the width (the present study),  $D_H = 4X_{in}$ . Based on  $X_{in}$ , the transition Froude number obtained by Friedman *et al.* [11] is  $Fr \approx 1.0$ .

In the numerical investigations of Srinarayana *et al.* [8], the critical Froude number for an unsteady fountain at full development was  $Fr = 2.25$  at  $Re = 100$ , while in the current work for the same Reynolds number the critical Froude number is  $Fr \approx 1.0$ . It is noted that Srinarayana *et al.* [8] used a uniform velocity profile at the fountain inlet whereas in the current work parabolic velocity profile has

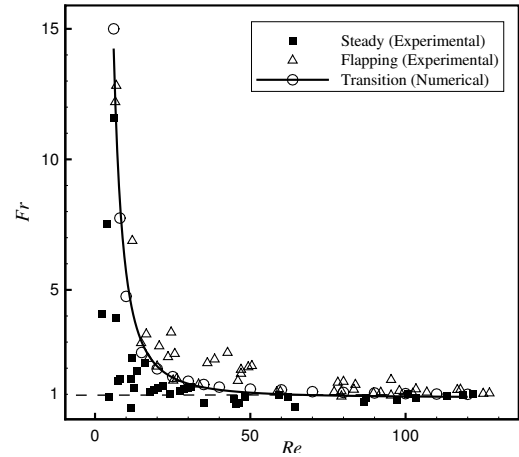


Figure 5:  $Re - Fr$  plane.

been used. For a given flow rate, fountains with parabolic velocity profile have higher momentum flux compared to fountains with uniform velocity inlet profile, and thus parabolic velocity inlet profile fountains would be expected to become unstable at a lower Froude number for the same Reynolds number.

## Conclusions

The behavior of plane fountains at low-Reynolds number has been investigated numerically. The critical Froude number for transition from steady to unsteady behavior at full development was mapped on to a  $Re - Fr$  plot and was found to vary with the Reynolds number. For  $Re > 60$ , the critical Froude number was found to remain nearly constant at  $Fr \approx 1.0$ , and for lower Reynolds number  $Re \leq 50$  there was a significant increase in the transition Froude number. The critical  $Fr$  line was well approximated by  $Fr \sim 0.95 + 481Re^{-2}$ . The fountains below and to the left of this demarcation line were completely steady and symmetric about the fountain source at full development. The fountains above and to the right of this demarcation line were unsteady and exhibit flapping behavior with repeated sideways shedding and rising of the top of the fountain. The behaviour of steady and flapping fountains was also observed in the non-dimensional fountain

height. The transition Froude numbers obtained in the present work match well with previous experimental work and open the way for investigation into fountain behaviour at very low Reynolds number ( $Re \ll 5$ ) and into the creeping flow regime.

### Acknowledgements

The support of the Australian Research Council is gratefully acknowledged.\*

### References

- [1] B. R. Morton, Forced Plumes, *J. Fluid Mech.*, **5**, 1959, 151–163.
- [2] I. H. Campbell, J. S. Turner, Fountains in magma chambers, *J. Petrol.*, **30**, 1989, 885–923.
- [3] W. D. Baines, J. S. Turner, I. H. Campbell, Turbulent fountains in an open chamber, *J. Fluid Mech.*, **212**, 1990, 557–592.
- [4] N. Williamson, N. Srinarayana, S.W. Armfield, G. McBain, W. X. Lin, Low Reynolds number fountain behaviour, *J. Fluid Mech.*, **608**, 2008, 297–317.
- [5] W. X. Lin, S. W. Armfield, Direct simulation of weak laminar plane fountains in a homogeneous fluid, *Int. J. Heat Mass Transfer*, **43**, 2000, 3013–3026.
- [6] W. X. Lin, S. W. Armfield, The Reynolds and Prandtl number dependence of weak fountains, *Comput. Mech.*, **31**, 2003, 379–389.
- [7] N. Srinarayana, N. Williamson, S. W. Armfield, W. X. Lin, Line fountain behavior at low-Reynolds number, *Int. J. Heat Mass Transfer*, **53**, 2010, 2065–2073.
- [8] N. Srinarayana, G. D. McBain, S. W. Armfield, W. X. Lin, Height and stability of laminar plane fountains in a homogeneous fluid, *Int. J. Heat Mass Transfer*, **51**, 2008, 4717–4727.
- [9] S. Popinet, Gerris: a tree-based adaptive solver for the incompressible Euler equations in complex geometries, *J. Comput. Phys.*, **190**, 2003, 572–600.
- [10] D. Goldman, Y. Jaluria, Effect of opposing buoyancy on the flow in free and wall jets, *J. Fluid Mech.*, **166**, 1986, 41–56.
- [11] P. D. Friedman, V. D. Vadakoot, W. J. Meyer Jr, S. Carey, Instability threshold of a negatively buoyant fountain, *Exp. Fluid*, **42**, 2007, 751–759.